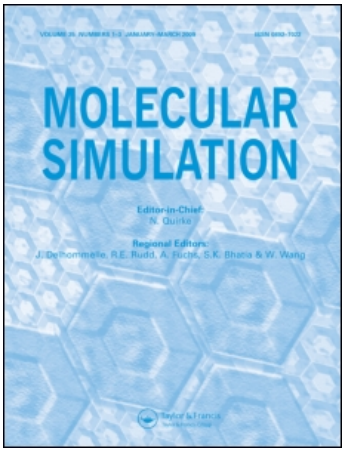

Molecular Simulation
Publication details, including instructions for authors and subscription information:
http://www.informaworld.com/smpp/title~content=t713644482

Molecular modelling of *Mycobacterium tuberculosis* acetolactate synthase catalytic subunit and its molecular docking study with inhibitors

Thais C. S. Souza[a]; Daniela Josa[a]; Teodorico C. Ramalho[a]; Melissa Soares Caetano[a]; Elaine F. F. da Cunha[a]
[a] Departamento de Química, Universidade Federal de Lavras, Lavras, MG, Brazil

To cite this Article Souza, Thais C. S. , Josa, Daniela , Ramalho, Teodorico C. , Caetano, Melissa Soares and da Cunha, Elaine F. F.(2008) 'Molecular modelling of *Mycobacterium tuberculosis* acetolactate synthase catalytic subunit and its molecular docking study with inhibitors', Molecular Simulation, 34: 7, 707 — 713
To link to this Article: DOI: 10.1080/08927020802129974
URL: http://dx.doi.org/10.1080/08927020802129974

Molecular Simulation
Vol. 34, No. 7, June 2008, 707–713

Taylor & Francis
Taylor & Francis Group

Molecular modelling of *Mycobacterium tuberculosis* acetolactate synthase catalytic subunit and its molecular docking study with inhibitors

Thais C.S. Souza, Daniela Josa, Teodorico C. Ramalho, Melissa Soares Caetano and Elaine F.F. da Cunha*

Departamento de Química, Universidade Federal de Lavras, Lavras, MG, Brazil

(*Received 16 February 2008; final version received 13 April 2008*)

Mycobacterium tuberculosis is a leading cause of infectious disease in the world today. This outlook is aggravated by a growing number of *M. tuberculosis* infections in individuals who are immunocompromised as a result of HIV infections. Thus, new and more potent anti-TB agents are necessary. Therefore, acetolactate synthase (*mt*ALS) was selected as a target enzyme to combat *M. tuberculosis*. In this work, the three-dimensional molecular model of the hypothetical structure for the ALS catalytic subunit of *M. tuberculosis* was elucidated by homology modelling. In addition, the orientations and binding affinities of sulfonylurea inhibitors with the new structure was investigated. Our findings could be helpful for the design of new, more potent mtAHAS inhibitors.

Keywords: homology modelling; molecular docking; sulphonylureas; *Mycobacterium tuberculosis* acetolactate synthase

1. Introduction

Acetolactate synthase (ALS; also known as acetohydroxyacid synthase; EC 2.2.1.6) is the first common enzyme in the biosynthetic pathway of the branched-chain amino acids in bacteria, fungi and higher plants [1]. The enzyme catalyses two parallel reactions: the condensation of two pyruvate molecules to give rise to 2-acetolactate in the first step of the valine and leucine synthetic pathway, and the condensation of pyruvate and 2-oxobutyrate to yield 2-aceto-2-hydroxybutyrate in the second step of isoleucine biosynthesis [2]. Thiamin diphosphate (ThDP) is the cofactor of this enzyme and coordinates to a divalent metal ion such as Mg^{2+}. In addition, ALS also binds a molecule of flavin adenine dinucleotide (FAD), although this cofactor is unusual because the reactions catalysed by ALS involve no net reduction or oxidation [3]. Bacterial ALSs are composed of large and small subunits, in an $\alpha 2\beta 2$ heterotetramer. It has been generally accepted that the large (60–70 kDa) subunits are catalytic, where pairs of catalytic subunits form an intimate dimer containing two active sites. The small ones are regulatory (9.5–54 kDa) [4]. The molecular size of the plant and fungal enzymes is less certain and the enzymes, as isolated, frequently contain the catalytic subunits only [5].

ALS constitutes a target for five structurally diverse inhibitor classes: sulphonylureas, imidazolinones, triazolopyrimidines, pyrimidinylthio (or oxy)-benzoates and sulphonylamino-carbonyltriazolinones [1]. The sulphonylurea herbicides were discovered by Levitt et al. and the most active compounds show an aromatic ring attached to the sulphur atom and a heterocyclic ring (pyrimidine or triazine) attached to the distal nitrogen atom. The most known are: pyrazosulfuron ethyl (PSE), primisulfuron methyl (PSM), sulfometuron methyl (SM), metsulfuron methyl (MM), chlorimuron ethyl (CE), chlorsulfuron (CS), thifensulfuron methyl (TM), nicosulfuron (NS) and triasulfuron (TS). The sensitivity of ALS to the different sulphonylureas varies substantially. For example, Duggleby et al. have purified the wild-type and mutant yeast ALS and determined their sensitivity to six sulphonylureas [6]. Yeast ALS showed apparent K_i values of 3.25 (CE), 5.08 (SM), 9.40 (MM), 5.25 (TM) and 127.0 nM (CS). They observed that yeast ALS has an extended N-terminal sequence that is not present in bacterial ALS. Additionally, Chang et al. expressed, purified and characterised the *Arabidopsis thaliana* ALS and observed that it is strongly inhibited by the sulphonylurea herbicides [7,8]. *A. thaliana* ALS showed apparent K_i values of 10.8 (CE), 25.5 (SM), 36.2 (MM), 72.2 (TM) and 54.6 nM (CS). Choi et al. searched the inhibitory activities of various sulphonylurea herbicides against the catalytic subunit of *Mycobacterium tuberculosis* acetolactate synthase (*mt*ALS). They suggested that ALS might serve as a target protein for the development of novel anti-tuberculosis therapeutics [9,10].

M. tuberculosis is a leading cause of morbidity and mortality in the world today [11–13]. This fact is aggravated by a growing number of Mtb infections in individuals who are immunocompromised as a result of HIV infections [14]. In addition, the ongoing selection

*Corresponding author. Emails: elaine_cunha@ufla.br; effcid@dacafe.com

ISSN 0892-7022 print/ISSN 1029-0435 online

DOI: 10.1080/08927020802129974
http://www.informaworld.com

of multiple drug resistant and extensively drug resistant strains of *M. tuberculosis* has markedly reduced the effectiveness of the standard treatment regimens. Thus, there is an urgent need for new drugs that are potent inhibitors of *M. tuberculosis*. Therefore, in this paper, we described the three-dimensional molecular model of *mt*ALS catalytic subunit obtained through the use of the homology modelling technique. In addition, we investigated the orientations and binding affinities of some sulpfonylureas with this new structure.

2. Methodology

2.1 Sequence alignment

The amino acid primary sequence of *mt*ALS was retrieved from the Swiss-Model Data Bank [15–18]. This program manipulates and compares proteins and sequences for homology modelling. As a first approach, an extensive search of potential templates for the *mt*ALS protein was carried out. The search for sequences similar to *mt*ALS within the Protein Data Bank (PDB) [19] was performed with the Basic Local Alignment Search Tool program [20]. The search for the best template for modelling was carried out by choosing structures possessing a high degree of sequence similarity with *mt*ALS. The crystal structural coordinates of *A. thaliana* (PDB code: 1Z8N and 1YBH) [21] and *Sacharomyces cerevisiae ALSs* (PDB code: 1T9C) [22] were used as template structure to build a three-dimensional model of *mt*ALS. Sequence alignment was performed using ClustalW [21] and then adjusted in according to Delfino et al. [23].

2.2 Model building, refinement and evaluation

An automated homology model was performed using the Geno3D, an automatic web server for protein molecular modelling [24]. After identifying homologous proteins and performing the alignment of both template and target sequences, it extracted geometrical restraints (dihedral angles and distances) for corresponding atoms between the query and the template and performed the three-dimensional construction of the protein by using a distance geometry approach.

Hydrogen atoms were added to the modelled structure and the atomic coordinates were minimised by the use of the following protocol, to which constraints and restraints were added in order to gain better control over structure relaxation [11]. The protocol included four successive steps: (i) to eliminate the initial strains, only hydrogen atoms were allowed to move, while the heavy atoms were kept fixed; (ii) for the next adjustments, the enzyme side-chains were tether restrained, keeping the main-chain atoms fixed; (iii) the tethering restraints for the backbone atoms were gradually decreased and (iv) strains were minimised until the system was completely relaxed. One thousand steepest descent minimisation steps were carried out, followed by the conjugate gradient minimisation method, until the derivatives were of the order of 5.0, 1.0 and 0.5 $kJ\,mol^{-1}\,Å^{-1}$.

The dimmer was modelled based on the crystal structure yeast ALS (code PDB: 1JSC). FAD, Mg and ThDP were added to the enzyme previously aligned with 1JSC. After that, the complex was slowly relaxed to clean the starting structure, according to a protocol similar to the one used with the template structures. Those steps were necessary to remove bad contacts or internals in the initial rigid structure, to reduce distortion risks and to lead to an optimised starting point for the subsequent docking calculations. The molecular dynamics simulations were carried out in vacuum following standard MD protocol, e.g. $T = 300$ K, 10,000 ps equilibration and 1 fs integration time with no cut-off for long-range interactions. A distance-dependent dielectric constant was applied to avoid overestimated charge–charge effects [25].

2.3 Validation of model

Validation of the generated model was done with the Procheck and Whatif available in the Biotech Validation Suite for Protein Structure (http://biotech.ebi.ac.uk:8400/) [26]. The superposition between the backbone of template and target enzymes was available using the Swiss-Pdb Viewer 3.7 program [27].

2.4 Ligands data set

Three-dimensional structures of each of the nine compounds (Figure 1) were based on the bioactive conformation of CE co-crystallised with *A. thaliana* ALS (PDB – Code PDB: 1YBH), and were built using the PC Spartan program Pro/Builder module [28]. Subsequently, the overall geometry optimisations and partial atomic charge distribution calculations of the ligands were performed with the same program using the AM1 semi-empirical molecular orbital method [29].

2.5 Docking studies

The compounds were docked into the *mt*ALS binding site using the Molegro Virtual Docker (MVD) [30], a program for predicting the most likely conformation of how a ligand will bind to a macromolecule. Ligand and protein are considered flexible during the docking simulation.

The MolDock scoring function used by MVD is derived from the piecewise linear potential (PLP), a simplified potential whose parameters are fit to protein–ligand structures and binding data scoring functions and further extended in Generic Evolutionary Method for

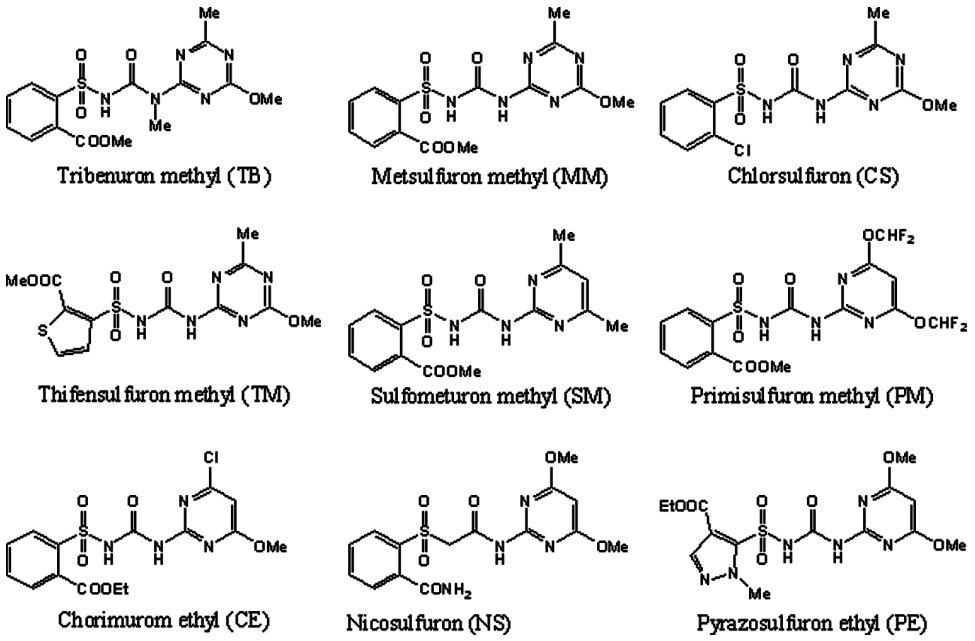

Figure 1. Sulphonylureas inhibitors.

molecular DOCK with a new hydrogen bonding term and new charge schemes [30]. The docking scoring function, E_{score}, is defined by the following energy terms:

$$E_{\text{score}} = E_{\text{inter}} + E_{\text{intra}}, \tag{1}$$

where E_{inter} is the ligand–protein interaction energy:

$$E_{\text{inter}} = \sum_{i\in\text{ligand}} \sum_{j\in\text{protein}} \left[E_{\text{PLP}}(r_{ij}) + 332.0 \frac{q_i q_j}{4r_{ij}^2} \right]. \tag{2}$$

The E_{PLP} term is a 'piecewise linear potential' using two different sets of parameters: one set for approximating the steric (van der Waals) term between atoms, and another stronger potential for hydrogen bonds. The second term describes the electrostatic interactions between charged atoms. It is a Coulomb potential with a distance-dependent dielectric constant given by: $D(r) = 4r$. The numerical value of 332.0 adjusts the units of the electrostatic energy to kilocalories per mole [30].

E_{intra} is the internal energy of the ligand:

$$E_{\text{intra}} = \sum_{i\in\text{ligand}} \sum_{j\in\text{ligand}} E_{\text{PLP}}(r_{ij}) + \sum_{\text{flexible bonds}} A[1 - \cos(m\cdot\theta - \theta_0)] + E_{\text{clash}}. \tag{3}$$

The first term (double summation) is between all atom pairs in the ligand excluding atom pairs which are connected by two bonds. The second term is a torsional energy term, where θ is the torsional angle of the bond. The average of the torsional energy bond contribution is used if several torsions could be determined. The last term, E_{clash}, assigns a penalty of 1000 if the distance between two heavy atoms (more than two bonds apart) is less than 2.0 Å, ignoring infeasible ligand conformations [30]. Summarising, these functions are used to automatically superimpose a flexible molecule onto a rigid template molecule.

The docking search algorithm used in MVD is based on an evolutionary algorithm, where interactive optimisation techniques inspired by Darwinian evolution theory, and a new hybrid search algorithm called guided differential evolution. The guided differential evolution algorithm combines the differential evolution optimisation technique with a cavity prediction algorithm during the search process, which allows for a fast and accurate identification of potential binding modes (poses) [14,31,36].

The active site exploited in docking studies was defined, with a subset region of 13.0 Å from the centre of the ligand. The interaction modes of the ligand with the *mt*ALS active site were determined as the highest energy scored protein–ligand complex used during docking and the conformers of each compound mostly associated with bioactive conformations of SM.

Finally, we calculated the highest occupied molecular orbital (HOMO) and lowest unoccupied molecular orbital (LUMO) energy values at Hartree–Fock level with 6-31G of conformer selected of each compound obtained in the docking studies [32]. HOMO has the priority to provide electrons, while LUMO accepts electrons first. According to the frontier molecular orbital theory, HOMO and LUMO are two important factors which affect the bioactivity of compounds [33]. A small difference between HOMO and LUMO implies high reactivity in reactions, while a large

difference between HOMO and LUMO implies low reactivity in reactions [34], because, in addition to the energy difference between HOMO and LUMO, the individual positions of those orbitals affect the reactivity. The calculations were performed using Gaussian 98 [35].

3. Results and discussion

3.1 Primary sequence comparison

As a first step, the alignment of the *mt*ALS primary structure with the chosen template sequences of 1Z8N, 1JCS and 1T9C was performed. The alignments of the primary structure between *mt*ALS and template sequence of 1Z8N, 1JCS and 1T9C showed 46.4, 46.4 and 44.5% identity, respectively.

3.2 Quality of the model

The Geno3D program [24] modelled two models based on the three templates: models 1 and 2. Table 1 shows the stereochemical quality (Ramachandran plot) of models. The compatibility between the active site of the *mt*ALS homology model, and the three-dimensional-structures of the templates used (1Z8N, 1JCS and 1T9C) were checked, superimposing the backbone of two enzymes (Table 1). Meaningful chain differences due to superimposition between models 1 and 2 were located in the sequence residues numbered 187 (5.86 Å), 223 (6.30 Å), 346 (5.57 Å), 359 (5.75 Å) and 360 (4.99 Å). So, we chose model 2 because it has the best stereochemical quality. FAD, Mg^{2+} and ThDP were added to model 2 and the complex was slowly relaxed to clean the starting structure. The stability of this model was then investigated by MD simulations in vacuum. The low energy conformation was therefore retained as the model 2a. Our final instigation from three-dimensional stereoscopic visual inspection is reproduced in Figure 2.

Table 1. Deviation among models and 1Z8N, 1YBH and 1T9C. Stereochemical quality (Ramachandran) of the proposed models.

	Model 1	Model 2
Deviation between models and 1Z8N (Å)	1.27	1.31
Deviation between models and 1YBH (Å)	1.23	1.32
Deviation between models and 1T9C (Å)	1.38	1.30
Deviation between models and model 1 (Å)	0.0	1.14
Deviation between models and model 2 (Å)	1.14	0.0
Ramachandran plot (%):		
Most favoured region	69.8	73.3
Allowed region	24.8	21.3
Generously allowed region	3.3	4.3
Disallowed region	2.1	1.0

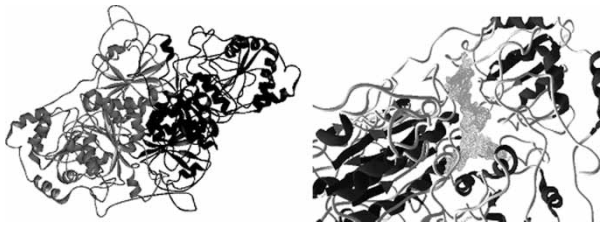

Figure 2. On the left, structure three-dimension of *mt*ALS dimer (black and grey) proposed by homology modelling. On the right, the *mt*ALS dimer with the cavity (hydrophobic tunnel).

3.3 Sulphonylureas docking orientation into mtALS

The docked binding mode is used to establish a link between the MolDock scoring function, structural properties of these compounds and their biological activity against the *mt*ALS [36, 37]. Evaluation of the docking results was based on protein–ligand complementarity considering steric and electrostatic properties. Additionally, we calculated the energy values for frontier orbitals (HOMO and LUMO) in order to verify the cation–π and π–π stacking interactions between enzyme and inhibitors, i.e. interactions between charged polar group and aromatic rings and interactions between aromatic rings, respectively.

The potential binding sites of *mt*ALS were calculated and a cavity of 278.0 A^3 (surface = 896.0 A^2) was observed close to Gly33, Ala34, Val108, Gly109, Phe118, Gln119, Lys168, Asp288, Arg289, Gly422, Leu423, Val484, Trp487, Ala563 and Ala564. The active site is located at the bottom of a hydrophobic tunnel (Figure 2).

After docking calculations, we verified that the orientation of the pyrimidine/triazine ring was similar to the observed binding mode of SM in the crystal structure of 1T9C for all compounds, except CE. Pyrimidine/triazine ring is oriented inside the tunnel, while the ring bonded to the sulphur atom is oriented to the tunnel surface, a region accessible to the solvent. Three orientations of the ring bonded to the sulphur atom were presented: the first formed for compounds CS, MM and TM, all with triazine ring. The second formed for compounds NS, PSE, PSM and TB, and the last formed for compound SM (Figure 3). The pyrimidine ring of CE superimposes well with the aromatic ring bonded to the sulphur atom of SM (crystal), thus it was just one compound with an orientation contrary to the other compounds in the active site. The substituent $-COOCH_2CH_3$ of CE is bulkier than the other substituents at the *ortho* position in the others, so we believe that there is a hindrance between $-COOCH_2CH_3$ and the position occupied inside the active site for other substituents.

We calculated the following parameters, as shown in Table 2: (a) energy score values used during docking; (b) interaction energy between ligand and the cofactor; (c) interaction energy between ligand and protein; (d) internal energy values of ligand and (e) hydrogen bonding energy values. It is evident from Table 2 that the difference between

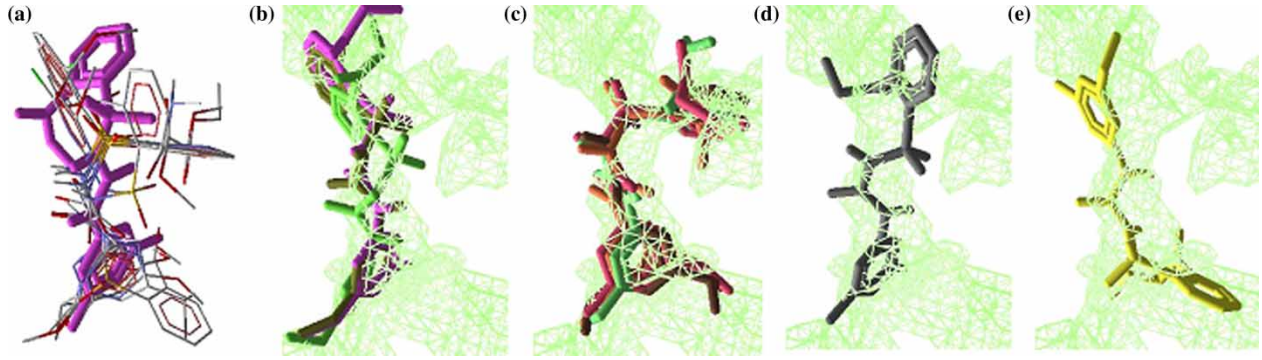

Figure 3. (a) Superposition between SM crystal (pink) and nine compound. (b) Superposition between MM (pink), CS (green) and TM (dark green) docked into the cavity of *mt*ALS (green). (c) Superposition between TB (pink), PSM (brown), PSE (orange) and NS (green) docked into the cavity (green). (d) SM docked into the cavity (green). (e) CE docked into the cavity (green).

Table 2. Estimated energy score (kcal mol^{-1}) values (MolDockScore) used for the evaluation of docking poses; total interaction energy (kcal mol^{-1}) values between the pose and the target molecule, interaction energy (kcal mol^{-1}) values between the cofactor and the target molecule; intramolecular energy values and hydrogen bond energy (kcal mol^{-1}) values between the nine sulphonylureas inhibitors and *mt*ALS enzyme.

Name	MolDockScore	Intermolecular energy	Intramolecular energy	Cofactor	HBond
PSE	− 170.09	− 151.47	− 8.79	− 7.32	− 13.94
PSM	− 164.49	− 153.46	− 0.80	− 7.73	− 6.76
NS	− 157.14	− 147.14	0.62	− 8.16	− 10.24
MM	− 155.85	− 150.16	5.02	− 8.22	− 8.94
TB	− 151.76	− 141.83	0.82	− 10.74	− 8.78
CE	− 146.60	− 144.87	8.82	− 10.56	− 16.34
TM	− 144.78	− 132.27	− 4.51	− 6.54	− 20.20
CS	− 139.95	− 131.3	2.38	− 8.48	− 7.35
SM	− 126.15	− 123.20	6.93	− 7.39	− 5.31

energy scores of the compounds increase following the tendency PSE < PSM < NS < MM < TB < CE < TM < CS < SM, i.e. PSE interacts more strongly with *mt*ALS than others compounds. According to Choi et al. [9], PSE ($IC_{50} = 0.87\ \mu M$), PSM ($IC_{50} = 4.19\ \mu M$), MM ($IC_{50} = 5.96\ \mu M$) and CE ($IC_{50} = 8.97\ \mu M$) inhibited more than 80% of the activity at 40 μM of *mt*ALS catalytic subunit, while CS and TM inhibited less than 10% at 40 μM. Thus, our theoretical results corroborated with experimental data. Analysing the hydrogen bond formed between the nine compound and *mt*ALS we observed: (i) all compounds interact with Arg289A; (ii) all compounds, except SM, interacted with Lys168B; (iii) all compounds, except PSM, interacted with Ala34B; (iv) all compounds, except PSM, interacted with Ala34B; (v) only TM exhibited a hydrogen bond with Gly109B and (vi) only PSE and PSM exhibited hydrogen bonds with Ala564A. Figure 4 shows PSE inside the *mt*ALS active site and the amino acid residues that interact through hydrogen bonds. The nine compounds interact with Arg289 forming at least two hydrogen bonds. This happens because the two rings of each compound interact with this amino acid, thus the conformation of sulphonylureas adopted in the *mt*ALS is addressed by Arg289.

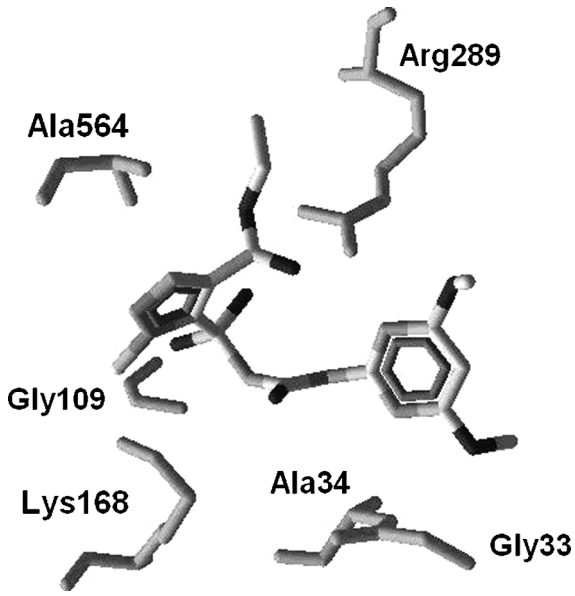

Figure 4. Docked structure of compound PSE into the *mt*ALS active site. The residues shown are involved in hydrogen bonding with the nine compounds.

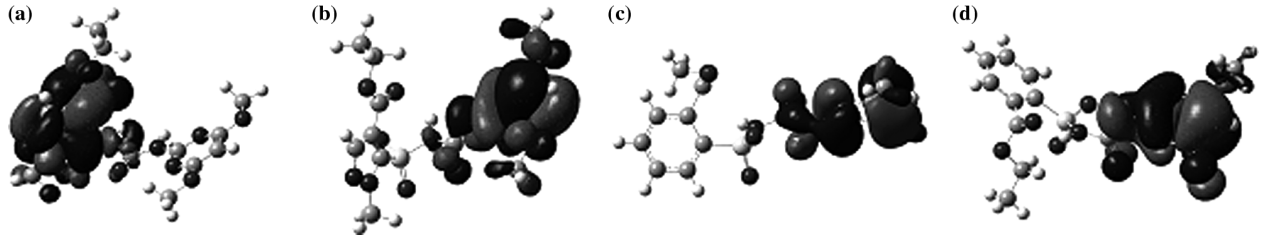

Figure 5. Molecular orbital surfaces: (a) HOMO–PSE; (b) LUMO–PSE; (c) HOMO–SM and (d) HOMO–CE.

The HOMO–LUMO three-dimensional shapes were examined and the data obtained show that HOMO of all compounds, except CE and SM, are localised on the ring bonded to sulphur atom, it is important to note that LUMO is located on the pyrimidine/triazine ring (Figure 5). These data were expected because the HOMO is in the electron-rich portion (sulphonamide bridge) and the LUMO is in electron-poor region (heterocyclic). However, HOMO of SM and CE are localised on the pyrimidine ring and the LUMO on the ring bonded to sulphur atom. We believe the absence of electronegative substituents at the pyrimidine ring of SM increases the electronic density in this ring because methyl substituents inductively donate electrons. The orientation of the CE conformer selected is different from other compounds, so, it is worth to note, the HOMO shape is located in the same region as the other compounds in relation to protein. In fact, as discussed previously, we observe that the pyrimidine/triazine ring is oriented inside the tunnel, while the ring bonded to the sulphur atom is oriented to the tunnel surface. We can thus propose that the conformational preference of the sulphonylureas inhibitors is likely due to interaction of LUMO (from inhibitor) and HOMO (from Trp487) orbital.

4. Conclusion

We carried out three-dimensional molecular model of the *mt*ALS hypothetical structure using homology modelling technique and molecular docking studies in order to understand the interaction of a series of sulphonylureas with it. Docked structures were evaluated based on intermolecular/intramolecular energies and hydrogen bonding interactions and the results combined with experimental data for inhibition of the *mt*ALS. It is possible that sulphonylureas analogs might be used as potential *mt*ALS inhibitors and a pyrazole ring bonded to sulphur atom increases the potency of these analogs. Considering that the emergence of resistant strains of *M. tuberculosis* poses a serious threat to the control of this disease, *mt*ALS is a possible new target to combat tuberculosis. Finally, our findings also suggest the importance of the location of the frontier orbital (HOMO and LUMO) of the studied sulphonylureas inhibitors. The HOMO of all compounds is localised on the ring bonded to sulphur atom, while LUMO is located on the pyrimidine/triazine ring. Probably, the orientation of the inhibitors in the active site is governed by interaction between the HOMO and LUMO orbitals. This study may be helpful in understanding the molecular interactions and the structural factors responsible for the activity of new ALS inhibitors targeting *M. tuberculosis*.

Acknowledgements

We are grateful to the FAPEMIG and CNPq Brazilian agencies for funding part of this work.

References

[1] Q. Zhou, W. Liu, Y. Zhang, and K.K. Liu, *Action mechanisms of acetolactate synthase-inhibiting herbicides*, Pest. Biochem. Physiol. 89 (2007), pp. 89–96.
[2] Y. Zohar, M. Einav, D.M. Chipman, and Z. Barak, *Acetohydroxyacid synthase from* Mycobacterium avium *and its inhibition by sulfonylureas and imidazolinones*, Biochimica et Biophysica Acta 1649 (2003), pp. 97–105.
[3] J.A. McCourt, S.S. Pang, J. King-Scott, L.W. Guddat, and R.G. Duggleby, *Herbicide-binding sites revealed in the structure of plant acetohydroxyacid synthase*, PNAS 103 (2006), pp. 569–573.
[4] A. Kaplun, M. Vyazmensky, Y. Zherdev, I. Belenky, A. Slutzker, S. Mendel, Z. Barak, D.M. Chipman, and B. Shaanan, *Structure of the regulatory subunit of acetohydroxyacid synthase isozyme III from* Escherichia coli, J. Mol. Biol. 357 (2006), pp. 951–963.
[5] D.M. Chipman, R.G. Duggleby, and K. Tittmann, *Mechanisms of acetohydroxyacid synthases*, Curr. Opin. Chem. Biol. 9 (2005), pp. 475–481.
[6] R.G. Duggleby, S.S. Pang, and H. Yu, *Systematic characterization of mutations in yeast acetohydroxyacid synthase*, Eur. J. Biochem. 270 (2003), pp. 2895–2904.
[7] A.K. Chang and R.G. Duggleby, *Expression, purification and characterization of* Arabidopsis thaliana *acetohydroxyacid synthase*, Biochem. J. 327 (1997), pp. 161–169.
[8] ———, *Herbicide-resistant forms of* Arabidopsis thaliana *acetohydroxyacid synthase: Characterization of the catalytic properties and sensitivity to inhibitors of four defined mutants*, Biochem. J. 333 (1998), pp. 765–777.
[9] K. Choia, Y.G. Yub, H.G. Hahnc, J. Do Choid, and M. Yoon, *Characterization of acetohydroxyacid synthase from* Mycobacterium tuberculosis *and the identification of its new inhibitor from the screening of a chemical library*, FEBS Lett. 579 (2005), pp. 4903–4910.
[10] K. Choi, C.N. Pham, H. Jung, S. Han, J. Choi, J. Kim, and M. Yoon, *Expression of acetohydroxyacid synthase from* Bacillus anthracis *and its potent inhibitors*, Bull. Korean Chem. Soc. 27 (2006), pp. 1697–1701.
[11] E.F.F. da Cunha, T.C. Ramalho, and R.B. de Alencastro, *Interactions of 5-deazapteridine derivatives with* Mycobacterium

tuberculosis *and with human dihydrofolate reductases*, J. Biom. Struct. Dyn. 22 (2004), pp. 119–130.
[12] ———, *A density functional study on the complexation of ethambutol with divalent cations*, Theochem 676 (2004), pp. 149–153.
[13] E.F.F. da Cunha, T.C. Ramalho, R.B. de Alencastro, and E.R. Maia, *Docking simulations and QM/MM studies between isoniazid prodrug, catalase-peroxidase (KatG) and S315T mutant from* Mycobacterium tuberculosis, Comput. Math. Methods Med. 8 (2007), pp. 113–124.
[14] E.F.F. da Cunha, T.C. Ramalho, and R.C. Reynolds, *Binding mode analysis of 2,4-diamino-5-methyl-5-deaza-6-substituted pteridines with* Mycobacterium tuberculosis *and human dihydrofolate reductases*, J. Biomol. Struct. Dyn. 25 (2008), pp. 377–385.
[15] M.C. Peitsch, *Protein modeling by e-mail*, Bio/Technology 13 (1995), pp. 658–660.
[16] ———, *ProMod and Swiss-model: Internet-based tools for automated comparative protein modelling*, Biochem. Soc. Trans. 24 (1996), pp. 274–276.
[17] M.C. Peitsch and N. Guexjrnl, *SWISS-MODEL and the Swiss-PdbViewer: An environment for comparative protein modeling*, Electrophoresis 18 (1997), pp. 2714–2723.
[18] T. Schwede, J. Kopp, N. Guex, and M.C. Peitsch, *SWISS-MODEL: An automated protein homology-modeling server*, Nucleic Acids Res. 31 (2003), pp. 3381–3385.
[19] H.M. Berman, J. Westbrook, Z. Feng, G. Gilliland, T.N. Bhat, H. Weissig, I.N. Shindyalov, and P.E. Bourne, *The protein data bank*, Nucleic Acids Res. 28 (2000), pp. 235–242.
[20] S.F. Altschul, W. Gish, W. Miller, E.W. Myers, and D.J. Lipman, *Basic local alignment search tool*, J. Mol. Biol. 215 (1990), pp. 403–410.
[21] J.A. McCourt, S.S. Pang, J. King-Scott, L.W. Guddat, and R.G. Duggleby, *Herbicide-binding sites revealed in the structure of plant acetohydroxyacid synthase*, Proc. Natl Acad. Sci. USA 103 (2006), pp. 569–573.
[22] J.A. McCourt, S.S. Pang, L.W. Guddat, and R.G. Duggleby, *Elucidating the specificity of binding of sulfonylurea herbicides to acetohydroxyacid synthase*, Biochemistry 44 (2005), pp. 2330–2338.
[23] R.T. Delfino, O.A. Santos-Filho, and J.D. Figueroa-Villar, *Molecular modeling of wild-type and antifolate resistant mutant* Plasmodium falciparum *DHFR*, Biophys. Chem. 98 (2002), pp. 287–300.
[24] C. Combet, M. Jambon, G. Deléage, and C.A. Geourjon, *Geno3D: Automatic comparative molecular modelling of protein*, Bioinformatics 18 (2002), pp. 213–214.
[25] D.H.J. Mackay, A.J. Cross, and A.T. Hagler, in *Prediction of Protein Structure and The Principles of Protein Conformation*, G.D. Fasman ed., Plenum Press, New York, Ch. 7 1990, pp. 317–358.
[26] G. Vriend, *What if – a molecular modeling and drug design program*, Mol. Graph. 8 (1990), pp. 52–57.
[27] N. Guex, A. Diemand, M.C. Peitsch, and T. Schwede, GlaxoSmithKline R&D & the Swiss Institute of Bioinformatics.
[28] SpartanPro 1.0.1 Wavefunction, 2001.
[29] M.J.S. Dewar, E.G. Zoebisch, E.F. Healy, and J.J.P. Stewart, *AM1 – a new general-purpose quantum-mechanical molecular model*, J. Am. Chem. Soc. 107 (1985), pp. 3902–3909.
[30] R. Thomsen and M.H. Christensen, *MolDock: A new technique for high-accuracy molecular docking*, J. Med. Chem. 49 (2006), pp. 3315–3332.
[31] N. Schormanna, O. Senkovicha, S. Ananthanc, and D. Chattopadhyaya, *Docking and biological activity of pteridine analogs: Search for inhibitors of pteridine reductase enzymes from* Trypanosoma cruzi, J. Mol. Struct. (Theochem.) 635 (2003), pp. 37–44.
[32] R.R. Da Silva, T.C. Ramalho, and J.M. Santos, *On the limits of highest-occupied molecular orbital driven reactions: The frontier effective-for-reaction molecular orbital concept*, J. Phys. Chem. A 110 (2006), pp. 1031–1040.
[33] X. Liu, P. Chen, B. Wang, Y. Li, S. Wang, and Z. Li, *Synthesis, bioactivity, theoretical and molecular docking study of 1-cyano-N-substituted-cyclopropanecarboxamide as ketol-acid reductoisomerase inhibitor*, Bioorg. Med. Chem. Lett. 17 (2007), pp. 3784–3788.
[34] R. Galeazzi, C. Marucchini, M. Orena, and C. Zadra, *Molecular structure and stereoelectronic properties of herbicide sulphonylureas*, Bioorg. Med. Chem. 10 (2002), pp. 1019–1024.
[35] M.J. Frisch et al., Gaussian 98, revision A.11, Gaussian, Inc.: Pittsburgh, PA, 2001.
[36] D. Josa, E.F.F. da Cunha, T.C. Ramalho, T.C.S. Souza, and M.S. Caetano, *Homology modeling of wild-type, D516V and H526L* Mycobacterium tuberculosis *RNA polymerase and their molecular docking study with inhibitors*, J. Biomol. Struct. Dyn. 25 (2008), pp. 373–376.
[37] J.R. Pinheiro, M. Bitencourt, E.F.F. da Cunha, T.C. Ramalho, and M.P. Freitas, *Novel anti-HIV cyclotriazadisulfonamide derivatives as modeled by ligand- and receptor-based approaches*, Bioorg. Med. Chem. 16 (2008), pp. 1683–1690.